Climatically driven biogeographic provinces of Late Triassic tropical Pangea

Jessica H. Whiteside[a,1], Danielle S. Grogan[a], Paul E. Olsen[b,1], and Dennis V. Kent[b,c]

[a]Department of Geological Sciences, Brown University, 324 Brook Street, Box 1846, Providence, RI 02912; [b]Lamont-Doherty Earth Observatory, Columbia University, 61 Route 9W, Palisades, NY 10964; and [c]Department of Earth and Planetary Sciences, Rutgers University, Piscataway, NJ 08854

Contributed by Paul E. Olsen, March 3, 2011 (sent for review January 17, 2011)

Although continents were coalesced into the single landmass Pangea, Late Triassic terrestrial tetrapod assemblages are surprisingly provincial. In eastern North America, we show that assemblages dominated by traversodont cynodonts are restricted to a humid 6° equatorial swath that persisted for over 20 million years characterized by "semiprecessional" (approximately 10,000-y) climatic fluctuations reflected in stable carbon isotopes and sedimentary facies in lacustrine strata. More arid regions from 5–20°N preserve procolophonid-dominated faunal assemblages associated with a much stronger expression of approximately 20,000-y climatic cycles. In the absence of geographic barriers, we hypothesize that these variations in the climatic expression of astronomical forcing produced latitudinal climatic zones that sorted terrestrial vertebrate taxa, perhaps by excretory physiology, into distinct biogeographic provinces tracking latitude, not geographic position, as the proto-North American plate translated northward. Although the early Mesozoic is usually assumed to be characterized by globally distributed land animal communities due to of a lack of geographic barriers, strong provinciality was actually the norm, and nearly global communities were present only after times of massive ecological disruptions.

biotic provinciality | Cynodontia | orbital forcing | Procolophonidae | latitudinal gradient

Geographic and climatic barriers are among the main constraints on the distribution of organisms. During the Late Triassic, Pangea lacked significant geographic barriers nearly pole-to-pole, and was warm and equable without glaciation or sea ice (1). Nonetheless, when correlated temporally by nonbiostratigraphic means, diverse Late Triassic continental faunal and floral assemblages display dramatic differences across paleolatitude (e.g., refs. 2–4) (Fig. 1). Although the equator-to-pole temperature gradients may have been relatively weak, Milankovitch-type climatic variability expressed in precipitation and evaporation was nonetheless very important (5–8). Then, as now (9,10), this scale of temporal variability may have played a critical role in structuring terrestrial communities, and thus early Mesozoic sequences provide a unique window into the link between climate variability and biotic provinciality.

Here, we focus on the tropical regions of Late Triassic central Pangea and the role of traversodont cynodonts (basal synapsids) and procolophonids (parareptiles) as possible ecologically equivalent herbivores (Fig. 2) under different climatic regimes. We test the correlation between climate variability and biotic provinces within narrow swaths of time constrained by astrochronology, paleomagnetic polarity stratigraphy, and paleomagnetically determined plate position from long [>5 million years (My)] lacustrine and associated fluvial records spanning 30° of paleolatitude. We show that faunal composition tracks different modes of orbitally forced climate variability that maintained Pangean faunal provinces and suggest that this may be a common feature of continental ecosystems.

Geologic, Climatic, and Biotic Context

Exposed eastern North America rift basins, formed during the incipient breakup of Pangea, comprise a northeast-southwest transect across the paleo-equator and tropics (Fig. 1). Best known is the Newark basin that, during the approximately 32 My. covered by its continuously cored record (11, 12), translated northward with central Pangea, transecting zonal climate belts from the equator to 20°N (8, 13, 14). The astrochronologic and paleomagnetic polarity constraints on this sequence allow tight temporal calibration and correlation to other basin sections in eastern North America (Fig. 1). Perhaps because of the extreme continentality of the climate of Pangea or elevated temperatures associated with high atmospheric CO_2 concentrations (15, 16), these lacustrine records were extremely sensitive to insolation changes driven by celestial mechanics (6, 7, 17) as exemplified by the tropical (5–20°N) Newark basin lacustrine record displaying lake-level cycles with periods of approximately 20 thousand years (ky) (precession), approximately 100 ky (short eccentricity), and 405 ky (long eccentricity) (6). This record also reveals longer periods of climatic precession modulation of approximately 1.8 My and approximately 3.5 My cycles (7), but it notably lacks convincing obliquity periods (6), indicating that precession and eccentricity controlled lake-level cyclicity at these latitudes.

To examine the links between the expression of cyclical climate mode and biotic provinciality, we analyzed cores and measured outcrop sections in seven eastern North American rift basins from Nova Scotia to South Carolina, which together with the 20° of northward translation of the Newark basin extend the latitudinal transect an additional 5° south and 5° north, spanning a total of 30° of latitude (Fig. 1).

Many terrestrial vertebrates have been found in these rift basin sequences, including rich assemblages of hitherto unexpected composition (18). Most surprising are assemblages containing abundant small (skull length, 3–10 cm) traversodont cynodonts from multiple localities and levels within the Richmond and Deep River basins (Figs. 1 and 2) (e.g., refs. 18–20). Such assemblages were previously known exclusively from Gondwana (e.g., refs. 21, 22), and are still unknown from the American Southwest (23). Coeval strata from other eastern North America basins have produced assemblages of more familiar aspect, where procolophonid parareptiles of similar size to the cynodonts are abundant (24, 25). In these strata, traversodont cynodonts are either absent or very rare.

Traversodont cynodonts and procolophonids have dentitions that display at least superficially similar specializations for herbivory (25–27), consistent with a diet of tough, fibrous plant material (28, 29) (Fig. 2). Their mutually exclusive abundance patterns

Author contributions: J.H.W. designed research; J.H.W., D.S.G., P.E.O., and D.V.K. performed research; J.H.W. contributed new reagents/analytic tools; J.H.W., D.S.G., P.E.O., and D.V.K. analyzed data; and J.H.W. wrote the paper.

The authors declare no conflict of interest.

[1]To whom correspondence may be addressed. E-mail: Jessica_Whiteside@Brown.edu or polsen@ldeo.columbia.edu.

This article contains supporting information online at www.pnas.org/lookup/suppl/doi:10.1073/pnas.1102473108/-/DCSupplemental.

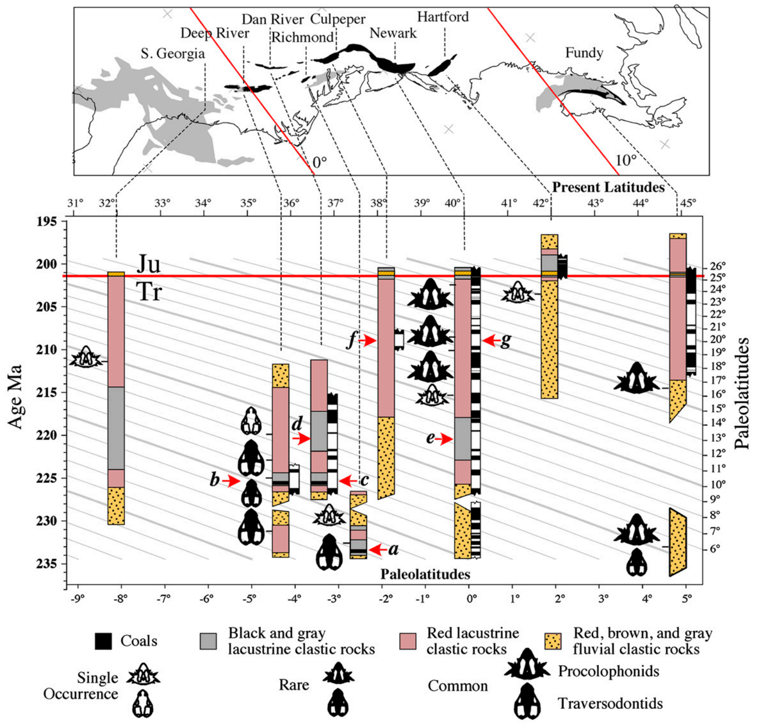

Fig. 1. (*Upper*) Map of basins studied. (*Lower*) Time-geography nomogram showing correlation of key rift basin sections in eastern North America, typical facies, and distribution of traversodonts and procolophonids. Time scale and paleolatitudes are based on the Newark basin section (6–8, 30). The gray curved lines are lines of equal paleolatitude assuming rift basins are within a rigid plate and all drift with Pangea. Red arrows show the position of the studied sections (*SI Text*): (*A*) Vinita Formation; (*B*) Cumnock Formation; (*C*) lower member Cow Branch Formation; (*D*) upper member Cow Branch Formation; (*E*) Lockatong Formation; (*F*) Balls Bluff Formation; (*G*) Passaic Formation.

and similar trophic adaptations suggest they could be ecological equivalents. Paleomagnetic polarity correlations (8, 11, 30, 31) and occurrences from multiple levels within several of these basins demonstrate that these disparate assemblages are broadly coeval, and that the traversodont-dominated assemblages occur in strata deposited within a few degrees of the equator, whereas procolophonid-dominated assemblages are found in higher tropical to subtropical latitudes. Thus, the differences between the assemblages suggest strong biotic provinciality, on a continent where an ambitious tetrapod could theoretically have walked from the Triassic location of Sydney to Vladivostok.

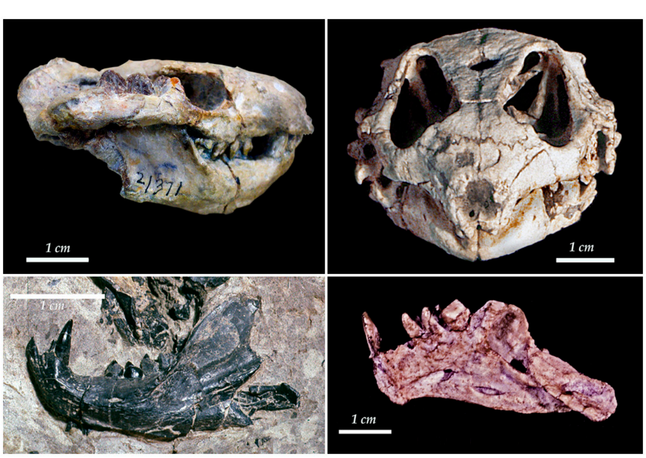

Fig. 2. Examples of traversodont cynodonts from equatorial latitudes (*Left*) and procolophonoid parareptiles from higher tropical latudes (*Right*). Skull is above, and mandible showing teeth is below. Scale bar, 1 cm. See *SI Text* for specimen data.

Core and Outcrop Materials

We analyzed lacustrine time series of environmental proxies from five basins and six lacustrine formations that collectively span a paleolatitudinal range of 17° and a temporal interval of 25 My (Figs. 1 and 3) from 209 to 234 Ma. Core and outcrop metadata are given in *SI Text* with ages based on the Newark basin astronomically tuned geomagnetic polarity time scale (Newark-APTS) correlation (32) (see *SI Text*). The environmental proxies used in our analyses are primarily related to lake depth and related ecosystem function (see *Methods*) that are in turn related to climate-driven water balance fluctuations. These include depth ranks (facies indicating different degrees of lake depth or desiccation), color (related to the redox state and organic carbon content of the sediment), total organic carbon (TOC—related to the redox state of the environment), and $\delta^{13}C_{toc}$ [related to the differential preservation of organic matter with different stable carbon isotopic ratios (33)].

Tropical Precessional Forcing

The records we examined were deposited in lakes in the tropics, and it is important to examine our expectations of orbitally forced water balance variability. Exactly what component of orbital forcing is important to water balance in the tropics is debatable (see ref. 34), but there is a growing consensus that the intensity of insolation drives the intensity of convection and hence precipitation in tropical monsoonal systems (34). Because the calendar date of the time of maximum precipitation is not constant, normal orbital solutions fixed to a date do not capture a time series of the intensity of maximum insolation.

In the tropics, the sun passes directly overhead both at the vernal and autumnal equinoxes, causing two warm and often two wet seasons. The position of the equinoxes with respect to perihelion gradually shifts over time, causing the two warm seasons to alternately coincide with annual maximum insolation (Fig. 4) (35). This coincidence occurs twice every precessional

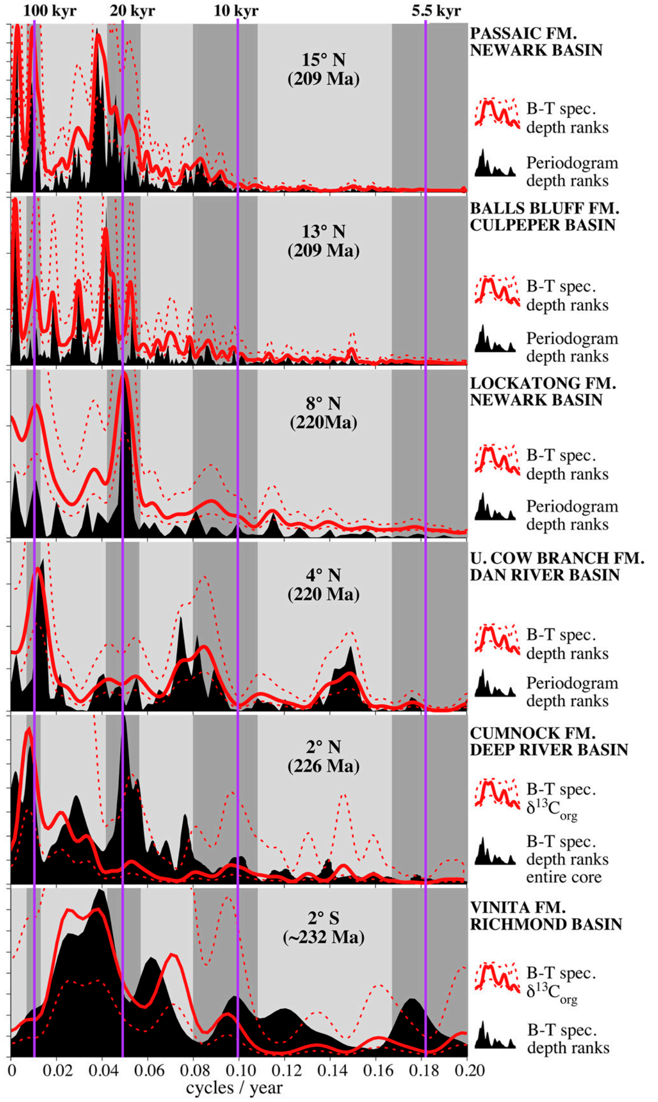

Fig. 3. Frequency spectra of the lacustrine sections. Measured sections and data curves of depth ranks, color, $\delta^{13}C_{org}$, and TOC are given in the *SI Text*. Darker gray bands show the range of frequencies expected for specific periods (purple).

cycle, resulting in an approximately 10-ky cycle (actually 9–12 ky) in tropical annual maximum insolation (Fig. 4) (35–37). Because at the tropics of Cancer and Capricorn the sun is directly overhead only once a year, the time of maximum insolation independent of the calendar date (Fig. 4) forms a clear latitudinally dependent pattern. At the equator, an approximately 10 ky cycle is present as well as a relative amplification of the spectral expression of the eccentricity cycles because of the asymmetry caused by "rectification" of the precession cycles induced in the insolation curve (36). This approximately 10-ky cycle is of precessional origin but has half-precessional periods, and it is termed semiprecession. Proceeding from the equator, the amplitude of the approximately 10-ky cycle and the eccentricity cycles decrease, whereas that of the familiar approximately 20-ky cycle increases, until the ~20-ky cyclicity dominates at the tropics and the ~10-ky cycle is absent (38). In as much as precipitation is coupled to convergence, lake high stands should be coupled to the period of maximum insolation. Therefore, in a monsoonal system we expect to see an approximately 10-ky cycle in lake depth within a few degrees of the equator.

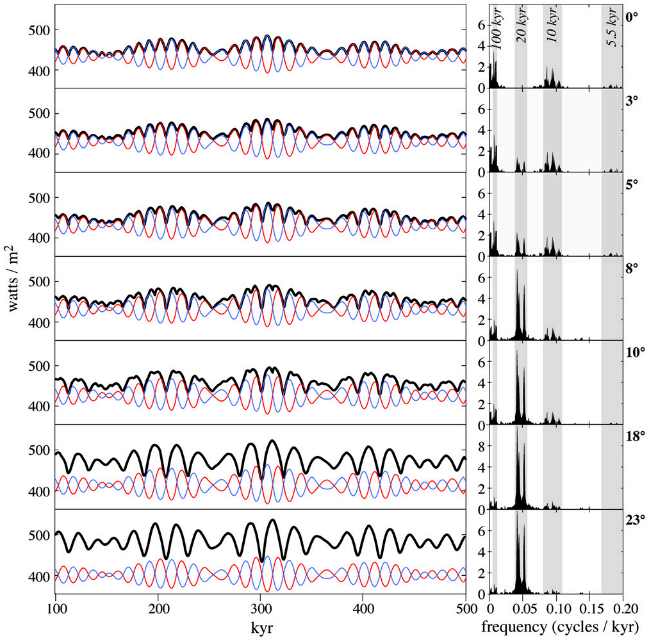

Fig. 4. (*Left*) Magnitude of maximum insolation (black), insolation at the vernal equinox (blue), and insolation at the autumnal equinox (red) from the equator to 23°N based on the La2004 solution (see *Methods*). (*Right*) Frequency spectra of maximum insolation showing the prevalent semiprecessional peak at frequency 0.10 near the equator, and the strong obliquity peak at frequency 0.05 farther north.

Energy balance models (36) and atmospheric general circulation models (34, 39, 40) capture this semiprecessional cycle in temperature and consequent precipitation variations, and both continental and marine Quaternary tropical climate records reveal at least a component of semiprecessional forcing (41–45). Increased temperature gradients caused by large northern hemisphere land masses enhance both the intensity and regional extent of precessional influences on hydrology in general circulation models (34), and therefore precessional and semiprecessional forcing of tropical hydrologic variations may have been enhanced during the Triassic existence of Pangea.

Spectral Results

The Richmond, Deep River, and Dan River basins' lacustrine records (Fig. 1) display periodicities consistent with orbital forcing within the available age model constraints including cycles of roughly 405-, 100-, and 20-ky period in all of the proxy records (Fig. 3), as do the Newark and Culpeper basins. However, the former three basins also contain strong approximately 10-ky to approximately 15-ky semiprecessional cycles. This semiprecessional cycle is stronger than the approximately 20-ky cycle in the Cow Branch Formation in the Dan River Basin, which is the equatorial section with the best temporal correlation to the Newark-APTS (see *SI Text* for details).

Our proxy time series tend to be highly asymmetrical, resembling a clipped precessional signal (see *SI Text*). Although power spectra of clipped precession signals can display artifactual semiprecession frequencies as result of the clipping itself, this is not the case in these data, because visual inspection shows peaks in the time series of the proxy data at the expected half cycle position, most apparent in direct comparison between the contemporaneous equatorial upper member of the Cow Branch Formation (4° N) and higher latitude Lockatong Formation (8°) (see *SI Text*). Other datasets show the same pattern as well, such as the taxonomic composition of palynomorph assemblages and organic matter type as seen in the Vinita Formation (46, 47). Thus, at the same time approximately 20-ky cycles dominated

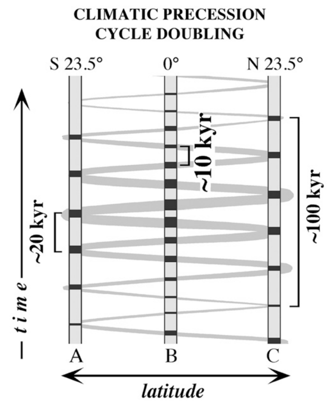

Fig. 5. Conceptual model showing relationship between the latitude of the coincidence of perihelion and the solstice through time. Width of the sinusoidal line is proportional to the insolation intensity at the coincidence of perihelion and solstice following the eccentricity cycles. *A*, *B*, and *C* represent hypothetical lacustrine sections showing lithological variations caused by lake level cycles produced by changes in precipitation tracking the yearly insolation maximum. *A* and *C* have pure approximately 20-ky cycles, whereas *B* at the equator has only an approximately 10-ky cycle.

the climate of the Newark basin region, approximately 10-ky cycles were dominant 4° to the south in the Dan River basin as predicted by local insolation forcing (Fig. 4) and our conceptual model (Fig. 5).

Discussion

The geographic pattern of periodicities seen in these Late Triassic rift basins corroborate the hypothesis that local forcing of climate, largely through the maximum intensity in insolation, independent of calendar date, controlled lake depth. The sections in the eastern North America Triassic rift basins with different modes of climate variability also have different faunas. The equatorial sections with relatively well-developed semiprecessional variability are dominated by traversondont cynodonts. But the sections deposited in higher tropical and subtropical latitudes not only show much weaker (or no) approximately 10-ky cyclicity, but also have different vertebrate assemblages characterized by abundant procolophonids, whereas traversodont cynodonts are virtually absent. A striking example is the higher paleolatitude (approximately 6°N), 233-Ma middle Wolfville Formation assemblage of the Fundy Basin. Abundant and diverse procolophonids occur in these fluvial strata and include the genera *Scoloparia*, *Acadiella*, and *Haligonia* (24). The only traversodont cynodont present is the rare and comparatively huge *Arctotraversodon* (dentary length = 40 cm) (ref. 48; H-D Sues, personal communication, 2010). Conversely, in the low paleolatitude Pekin (approximately 3°S) and Vinita (approximately 4°) formations, procolophonids are very rare, represented only by two specimens (49), among hundreds of specimens of the traversodont cynodont *Boreogomphodon* (50).

It is worth emphasizing that the approximately 10-ky cyclicity occurs at independently determined equatorial paleolatitudes where coals are preserved (5), along with the traversodont cynodonts. It is likely that the coupling of the double rainy season that is linked to the approximately 10-ky cyclicity with more intense equatorial insolation was responsible for the greater mean humidity and less intense dry periods of the region, which favored the traversodont cynodonts and coal formation. Support for this hypothesis that humidity was critical comes from Gondwanan high latitudes, where Late Triassic assemblages with abundant traversodont cynodonts also occur (4, 51). These specifically include the Ischigualastian assemblages of Argentina and the Santa Maria assemblages of Brazil associated with abundant gray, plant-bearing strata (52). Apparently, traversodont cynodonts had very disjunct ranges during the Late Triassic and were largely limited to humid zones. The distinct, apparently climate-related, provinciality of the Late Triassic is associated with high diversity globally, in dramatic contrast to the Early Jurassic in which global faunas are evidently homogenized, at least at higher taxonomic levels (2).

At a larger scale, floral data also shows a strong pattern of latitude-related provinciality, with time-transgressive microfloral assemblages being characteristic of low to higher latitudinal sedimentary basin successions (32) resulting from the northward translation of central Pangea, paralleling the pattern observed in larger vertebrates (2). Because the ranges of pollen and spores is often used for long range biostratigraphic correlation, there has been a strong tendency to conflate these biogeographic patterns with a biostratigraphic (i.e., temporal) signal in the absence, or even in the face of, strong, biostratigraphically independent means of temporal correlation (e.g., ref. 53).

The documentation of latitudinal separation of distinct vertebrate biotic provinces is consistent with the suggestion that Late Triassic archosaurs also show latitudinal differences (2, 4, 54, 55). These data show clear differences between taxa from the tropical semiarid zone of the American Southwest in comparison to the more humid high-latitude assemblages of South America. Astronomically forced latitudinal climate differences predict these observed differences and may indicate they were a major driver of Late Triassic terrestrial biogeography. More specifically, they also explain a long-standing puzzling pattern: the lack of traversodont cynodonts from fossiliferous strata in the American Southwest that were deposited north of the equatorial belt (13).

One possible mechanism limiting abundant traversodont cynodonts to equatorial and temperate latitudes might be their nitrogen excretion physiology. Synapsids, including humans and traversodonts, are ureotelic and retain the primitive tetrapod condition in which excreted urea is diluted by abundant water (56). In contrast, nearly all living sauropsids are uricotelic synthesizing uric acid (56), a feature likely present in procolophonids (see *SI Text*). The water used in synthesizing uric acid is recovered when it is precipitated prior to excretion, and hence, living sauropsids (including lizards and birds) tend to have an advantage over living synapsids—mammals—in water-poor areas. Thus, if procolophonids had sauropsid uricotely, they would be expected to be more successful at surviving water stress encountered not only seasonally, but more severely during the megadroughts at times of maximum precessional variability approximately every 20-ky cycle at extraequatorial tropical and subtropical latitudes. These arid intervals would be less extreme in the zone dominated by approximately 10-ky cyclicity. Because physiological water balance strategies are highly conserved among sauropsid and synapsid clades, this would be a likely mechanism to allow climate to sort the abundance of members of these clades, especially during extreme climate events.

Conclusions

Late Triassic equatorial Pangea lake levels followed an approximately 10-ky and approximately 20-ky cyclicity attributable to the control of precipitation by the doubling of the frequency of the climatic precession cycle. Contemporaneous lacustrine records from the higher latitude Newark basin show much less effect of the approximately 10-ky cycle and a correspondingly stronger ~20-ky cycle of "normal" climatic precession. The dominance of the ~20-ky cycle of climatic precession increased in younger strata as central Pangea drifted north during the Late Triassic (13). Biotic provinciality tracks the modes of climate variability with traversodont cynodont-dominated assemblages present in areas with ~10-ky cyclicity, whereas procolophonids are dominant in regions with the more familiar ~20-ky cyclicity. Even in a time of low equator-to-pole gradients, no ice, and no geographic barriers, Milankovitch variability, and climate in general, appears sufficient to have produced strong biotic provinciality. Physiological constraints acted on by climate extremes during times of high precessional variance may have been a key ecological structuring mechanisms. Biotic provinciality driven by zonal climate belts coupled with ecological incumbency, priority, or niche preemption effects (e.g., ref. 57) that develop as a consequence of the basic climatic structure may be prevalent when geographic barriers are minimal except at times of extreme ecological reorganization, such as the end-Permian (2, 58), and end-Triassic mass extinctions (2, 16) and the Paleocene-Eocene Thermal Maximum (59, 60) hyperthermal.

Methods

Depth Rank and Color. Depth rank, a proxy of relative lake depth, is a classification of facies by suites of sedimentary structures in which facies are assigned a value of 0 to 5 in order of increasing relative water depth (7, 17). Color is related to the reduction-oxidation state of the sedimentary environment.

Carbon Isotopic Analyses. From each section of interest, we took samples at submeter intervals for bulk carbon isotopic ($\delta^{13}C_{org}$) and TOC analyses. Samples were weighed into methanol-rinsed Ag boats, acidified in a desiccator over concentrated HCl for 72 h at 60–65 °C, dried for 24 h at 60–65 °C, and dried for an additional 24 h at 60–65 °C in a desiccator with silica gel. Samples were wrapped in Sn immediately prior to analysis. $\delta^{13}C_{org}$ and TOC measurements were made on a Costech 4010 Elemental Analyzer (EA) with a Zero-Blank carousel coupled to a Thermo DeltaVPlus stable light isotope ratio mass spectrometer (IRMS) at Brown University. Samples were flash-combusted in the EA at 1020 °C in a pure oxygen pulse, with resulting products being fully oxidized to CO_2 in a metal oxide bed, subsequent reduction of NO_x to N_2 in a copper bed, and chromatographic separation prior to admission to the IRMS. Standardization with reference pulses resulted in isotopic accuracy and precision better than 0.3% for CO_2.

Time Series Analysis. Time series analysis was performed using Analyseries 2.0.4.2 (61). The age models were developed either by direct correlation to the Newark-APTS by paleomagnetic polarity stratigraphy or by identification of one of the thickness periodicities as the 405-ky cycle of eccentricity (see *SI Text* for details).

Daily Insolation Model. For this model, daily solar insolation averaged over 24 h at latitude φ and day λ (rad, independent of calendar date) is given by (62, 63)

$$W = (S_0/\pi)\cdot[1+e\cos(\lambda\text{-}\omega\text{-}\pi)]^2/(1-e^2)^2 \cdot(H_0\sin\varphi\sin\delta+\cos\varphi\cos\delta\sin H_0), \quad [1]$$

where S_0 is the solar constant (1,365 W/m^2), H_0 is the hour angle, and δ is the declination angle. The orbital parameters of eccentricity e, obliquity ε, and precession ω are given by Laskar et al. (64) (abbreviated below as La2004) and provide

$$\sin\delta = \sin\varepsilon\sin\lambda \quad [2]$$

and

$$\cos H_0 = -\tan\varphi\tan\delta. \quad [3]$$

At the equator, maximum insolation occurs approximately at the equinoxes (vernal equinox, $\lambda = 0$; autumnal equinox, $\lambda = \pi$), and minimum insolation occurs approximately at the solstices (summer solstice, $\lambda = \pi/2$; winter solstice $\lambda = 3\pi/2$), although the exact values of maximum and minimum λ vary slightly over time (37). Moving away from the equator, maximum and minimum λ vary with increasing magnitude.

To find the magnitude and day of maximum and minimum insolation at latitude φ, we use a MATLAB program that implements Eq. **1** and the La2004 orbital parameter solution (SI Text). The program iteratively calculates daily solar insolation for $\lambda_{max} \pm$ d rad and $\lambda_{min} \pm$ d rad with steps of 0.02 rad, where λ_{max} and λ_{min} are the equinoxes and solstices, respectively. For φ < 10°, $d = 0.8$ is sufficient. For φ > 10°, d must increase with φ.

ACKNOWLEDGMENTS. We thank Carl Johnson for laboratory assistance. We are grateful to Sterling Nesbitt, Christine Janis, Bill Ryan, and two anonymous reviewers for helpful comments on earlier versions of this manuscript. We thank Robert J. Barron, Jack Boyland, Ted Daeschler, Andy Heckert, Vince Schneider, Joseph P. Smoot, and Hans-Dieter Sues for locality information. We thank the North Carolina and Virginia geological surveys for access to cores and permission to take samples. J.H.W. acknowledges support from the Richard Salomon Foundation and a National Science Foundation Advance award to Brown University, and P.E.O. is grateful for support from National Science Foundation Grant EAR 0753496.

1. Frakes LA, Francis JE, Syktus JL (1992) *Climate Modes of the Phanerozoic: The History of the Earth's Climate over the Past 600 Million Years* (Cambridge Univ Press, Cambridge, UK) p 274.
2. Shubin NH, Sues H-D (1991) Biogeography of early Mesozoic continental tetrapods: Patterns and implications. *Paleobiology* 17:214–230.
3. Olsen PE, Galton PM (1984) A review of the reptile and amphibian assemblages from the Stormberg of southern Africa, with special emphasis on the footprints and the age of the Stormberg. *Palaeontol Afr* 25:92–110.
4. Ezcurra MD (2010) Biogeographic analysis of Triassic tetrapods: Evidence for biotic provincialism and driven sympatric cladogenesis in the early evolution of modern tetrapod lineages. *Proc R Soc London Ser B* 277:2547–2552.
5. Olsen PE (1997) Stratigraphic record of the early Mesozoic breakup of Pangea in the Laurasia-Gondwana rift system. *Annu Rev Earth Planet Sci* 25:337–401.
6. Olsen PE, Kent DV (1996) Milankovitch climate forcing in the tropics of Pangea during the Late Triassic. *Palaeogeogr Palaeoclimatol Palaeoecol* 122:1–26.
7. Olsen PE, Kent DV (1999) Long-period Milankovitch cycles from the Late Triassic and Early Jurassic of eastern North America and their implications for the calibration of the early Mesozoic time scale and the long-term behavior of the planets. *Philos Trans R Soc A* 357:1761–1787.
8. Kent DV, Tauxe L (2005) Corrected Late Triassic latitudes for continents adjacent to the North Atlantic. *Science* 307:240–244.
9. Brown K, Ab'Sabar AH (1979) Ice age forest refuges and evolution in the Neotropics: Correlation of paleoclimatological, geomorphological, and pedological data with modern biological endemism. *Paleoclimas* 5:1–30.
10. Colinvaux PA, et al. (1996) A long pollen record from lowland Amazonia: Forest and cooling in glacial times. *Science* 276:85–88.
11. Kent DV, Olsen PE (1999) Astronomically tuned geomagnetic polarity time scale for the Late Triassic. *J Geophys Res* 104:12831–12841.
12. Kent DV, Olsen PE (2008) Early Jurassic magnetostratigraphy and paleolatitudes from the Hartford continental rift basin (eastern North America): Testing for polarity bias and abrupt polar wander in association with the central Atlantic magmatic province. *J Geophys Res* 113:B06105, 10.1029/2007JB005407.
13. Kent DV, Irving E (2010) Influence of inclination error in sedimentary rocks on the Triassic and Jurassic apparent pole wander path for North America and implications for Cordilleran tectonics. *J Geophys Res* 115:B10103, 10.1029/2009JB007205.
14. Kent DV, Olsen PE (2000) Magnetic polarity stratigraphy and paleolatitude of the Triassic-Jurassic Blomidon Formation in the Fundy basin (Canada): Implications for early Mesozoic tropical climate gradients. *Earth Planet Sci Lett* 179:311–324.
15. Schaller MF, Wright JD, Kent DV (2011) Atmospheric P_{CO_2} perturbations associated with the Central Atlantic Magmatic Province. *Science* 331:1404–1409.
16. McElwain JC, Beerling DJ, Woodward FI (1999) Fossil plants and global warming at the Triassic-Jurassic boundary. *Science* 285:1386–1390.
17. Olsen PE (1986) A 40-million-year lake record of early Mesozoic climatic forcing. *Science* 234:842–848.
18. Sues H-D, Olsen PE (1990) Triassic vertebrates of Gondwana aspect from the Richmond basin of Virginia. *Science* 249:1020–1023.
19. Olsen PE, Schneider V, Sues H-D, Peyer KM, Carter JG (2001) Biotic provinciality of the Late Triassic equatorial humid zone. *Geol Soc Am Abstracts with Programs* 33:A-27, Available at http://gsa.confex.com/gsa/2001SE/finalprogram/abstract_4541.htm.
20. Heckert AB, Schneider VP, Olsen PE, Mitchell JS (2009) Vertebrate diversity of the Upper Triassic Chatham Group, Deep River basin, central North Carolina. *Abstracts, Second Annual Meeting of the Southeastern Association of Vertebrate Paleontology* (Virginia Museum of Natural History, Martinsville, VA), p 8, Available at http://web.me.com/dooleyclan/SEAVP/SEAVP_files/Abstract%20book.pdf.
21. Sues H-D, Olsen PE, Carter JG (1999) A Late Triassic traversodont cynodont from the Newark Supergroup of North Carolina. *J Vertebr Paleontol* 19:351–354.
22. Romer AS (1966) *Vertebrate Paleontology* (University of Chicago Press, Chicago), 3rd Ed.
23. Irmis RB, Parker WG (2005) Unusual tetrapod teeth from the Upper Triassic Chinle Formation, Arizona, USA. *Can J Earth Sci* 42:1339–1345.
24. Sues H-D, Baird D (1998) Procolophonidae (Reptilia: Parareptilia) from the Upper Triassic Wolfville Formation of Nova Scotia, Canada. *J Vertebr Paleontol* 18:525–532.
25. Sues H-D, Olsen PE, Scott DM, Spencer PS (2000) Cranial osteology of *Hypsognathus fenneri*, a latest Triassic procolophonid reptile from the Newark Supergroup of eastern North America. *J Vertebr Paleontol* 20:275–284.
26. Gow CE (1977) Tooth function and succession in the Triassic reptile *Procolophon trigoniceps*. *Palaeontology* 20:695–704.
27. Carroll RL, Lindsay W (1985) Cranial anatomy of the primitive reptile *Procolophon*. *Can J Earth Sci* 22:1571–1587.
28. Crompton AW, Attridge J (1986) *The Beginning of the Age of Dinosaurs*, ed K Padian (Cambridge Univ Press, Cambridge, UK), pp 223–236.

29. Wing SL, Sues H-D (1992) *Terrestrial Ecosystems Through Time*, eds AK Behrensmeyer et al. (University of Chicago Press, Chicago), pp 327–360.
30. Kent DV, Olsen PE, Witte WK (1995) Late Triassic-Early Jurassic geomagnetic polarity and paleolatitudes from drill cores in the Newark rift basin (Eastern North America). *J Geophys Res* 100:14965–14998.
31. Kent DV, Olsen PE (1997) Magnetostratigraphy and paleopoles from the Late Triassic Dan River-Danville basin: Interbasin correlation of continental sediments and a test of the tectonic coherence of Newark rift basins in eastern North America. *Geol Soc Am Bull* 109:366–377.
32. Olsen PE, Kent DV, Whiteside JH (2011) Implications of the Newark Supergroup-based astrochronology and geomagnetic polarity time scale (Newark-APTS) for the tempo and mode of the early diversification of the Dinosauria. *Earth Environ Sci Trans R Soc Edinburgh*, (in press).
33. Whiteside JH, et al. (2011) Pangean great lake paleoecology on the cusp of the end-Triassic extinction. *Palaeogeogr Palaeoclimat Palaeoecol* 301:1–17.
34. Clement AC, Hall A, Broccoli AJ (2004) The importance of precessional signals in the tropical climate. *Clim Dynam* 22:327–341.
35. Berger A, Loutre MF, Mélice JL (2006) Equatorial insolation: From precession harmonics to eccentricity frequencies. *Clim Past*, 2 pp:131–136, Available at http://www.clim-past.net/2/131/2006/cp-2-131-2006.html.
36. Crowley TJ, Kim K-Y, Mengel JG, Short DA (1992) Modeling 100,000 year climate fluctuations in pre-Pleistocene series. *Science* 255:705–707.
37. Ashkenazy Y, Gildor H (2008) Timing and significance of maximum and minimum equatorial insolation. *Paleoceangraphy* 23:PA1206, 10.1029/2007PA001436.
38. Laepple T, Lohmann G (2009) Seasonal cycle as template for climate variability on astronomical timescales. *Paleoceanography* 24:PA4201, 10.1029/2008PA001674.
39. Liu Z, Harrison SP, Kutzbach J, Otto-Bliesner B (2004) Global monsoons in the mid- Holocene and oceanic feedback. *Clim Dynam* 22:157–182.
40. Kutzbach JE, Liu X, Liu Z, Chen G-S (2008) Simulation of the evolutionary response of global summer monsoons to orbital forcing over the past 280,000 years. *Clim Dynam* 30:567–579.
41. Lyons RP, et al. (2009) Scientific drilling in continental East Africa: The dominance of eccentricity modulated precession and half-precession on continental tropical climate. *Eos Trans Am Geophys Union* PP11B-1315.
42. Verschuren D, et al. (2009) Half-precessional dynamics of monsoon rainfall near the East African Equator. *Nature* 462:637–641.
43. Pokras EM, Mix AC (1987) Earth's precession cycle and Quaternary climatic change in tropical Africa. *Nature* 326:486–487.
44. Hinnov LA (2000) New perspectives on orbitally forced stratigraphy. *Annu Rev Earth Planet Sci* 28:419–475.
45. McIntyre A, Molfino B (1996) Forcing of Atlantic equatorial and subpolar millennial cycles by precession. *Science* 274:1867–1870.
46. Ediger VS (1986) Paleopalynological biostratigraphy, organic matter deposition and basin analysis of the Triassic-(?)Jurassic Richmond rift basin, Virginia USA. PhD dissertation (Pennsylvania State Univ, State College, PA), p 425.
47. Malinconico MAL (2002) Lacustrine organic sedimentation, organic metamorphism and thermal history of selected Early Mesozoic Newark Supergroup basins, Eastern USA. PhD thesis (Columbia Univ, New York), p 419.
48. Sues H-D, Hopson JA, Shubin NH (1992) Affinities of ?*Scalenodontoides plemmyridon* Hopson, 1984 (Synapsida: Cynodontia) from the Upper Triassic of Nova Scotia. *J Vertebr Paleontol* 12:168–171.
49. Sues H-D, Olsen PE (1993) A new procolophonid and a new tetrapod of uncertain, possibly procolophonian affinities from the upper Triassic of Virginia. *J Vertebr Paleontol* 13:282–286.
50. Sues H-D, Hopson JA (2010) Anatomy and phylogenetic relationships of *Boreogomphodon jeffersoni* (Cynodontia: Gomphodontia) from the Upper Triassic of Virginia. *J Vertebr Paleontol* 30:1202–1220.
51. Rogers RR, et al. (1993) The Ischigualasto tetrapod assemblage (Late Triassic, Argentina) and $^{40}Ar/^{39}Ar$ dating of dinosaur origins. *Science* 260:794–797.
52. Colombi CE, Parrish JT (2008) Late Triassic environmental evolution in southwestern Pangea: Plant taphonomy of the Ischigualasto Formation. *Palaios* 23:778–795.
53. Van Veen PM (1995) Time calibration of Triassic/Jurassic microfloral turnover, eastern North America—Comment. *Tectonophysics* 245:93–95.
54. Irmis RB, et al. (2007) A Late Triassic dinosauromorph assemblage from New Mexico and the rise of dinosaurs. *Science* 317:358–361.
55. Nesbitt SJ, et al. (2009) A complete skeleton of a Late Triassic saurischian and the early evolution of dinosaurs. *Science* 326:1530–1533.
56. Wright PA (1995) Nitrogen excretion: Three end products, many physiological roles. *J Exp Biol* 198:273–281.
57. Valentine JW, Jablonski D, Krug AZ, Roy K (2008) Incumbency, diversity, and latitudinal gradients. *Paleobiology* 34:169–178.
58. Huey RB, Ward PD (2005) Hypoxia, global warming, and terrestrial Late Permian extinctions. *Science* 308:398–401.
59. Zachos JC, et al. (2006) Extreme warming of mid-latitude coastal ocean during the Paleocene-Eocene Thermal Maximum: Inferences from TEX86 and isotope data. *Geology* 34:737–740.
60. Bowen GJ, et al. (2002) Mammalian dispersal at the Paleocene/Eocene boundary. *Science* 295:2062–2065.
61. Paillard D, Labeyrie L, Yiou P (1996) Macintosh program performs time-series analysis. *Eos Trans Am Geophys Union* 77:379.
62. Milankovitch M (1941) *Kanon der Erdbestrahlung und seine Andwendung auf das Eiszeitenproblem* (Royal Serbian Academy of Science, Belgrade).
63. Berger A (1978) Long-term variations of daily insolation and Quaternary climatic changes. *J Atmos Sci* 35:2362–2367.
64. Laskar J, et al. (2004) A long-term numerical solution for the insolation quantities of the Earth. *Astron Astrophys* 428:261–285.

GEOLOGY

EVOLUTION